Astron. Astrophys. 322, 565–575 (1997)

ASTRONOMY
AND
ASTROPHYSICS

Search for forced oscillations in binaries

II. β Scorpii A. New physical parameters and a search for line profile variability

D. Holmgren, P. Hadrava, P. Harmanec, P. Koubský, and J. Kubát

Astronomický ústav, Akademie věd České Republiky, 251 65 Ondřejov, Czech Republic
(david(had, hec, koubsky, kubat)@sunstel.asu.cas.cz)

Received 20 May 1996 / Accepted 8 November 1996

Abstract. We present new spectroscopic data and physical parameters for the early-type binary system β Sco A. Radial velocity measurements of Reticon spectra have been made using both cross-correlation and disentangling techniques. Spectroscopic orbits, based on the new data and published radial velocities are presented. The orbital period and apsidal motion rate have been refined using 603 radial velocities covering a time interval of 84 years. The anomalistic period is 6.828245 ± 0.000009 days, and the apsidal motion rate is $\dot{\omega} = 0.00131 \pm 0.00004$ degrees per day. The first visual - spectroscopic orbit for the system is given here as well, from which we derive a parallax for the system of $0\farcs0070 \pm 0\farcs0001$ corresponding to a distance of 143 ± 3 pc. This has allowed us to compute the absolute dimensions and mean internal structure constant for the system. We find, for the primary and secondary respectively, masses, radii, and effective temperatures of: $m_{\rm p}/m_{\odot} = 13.5 \pm 0.9$, $m_{\rm s}/m_{\odot} = 9.6 \pm 0.4$, $r_{\rm p}/r_{\odot} = 6.8 \pm 0.4, r_{\rm s}/r_{\odot} = 4.2 \pm 0.3, T_{\rm p} = 28000 \pm 2000$ K, and $T_{\rm s} = 26400 \pm 2000$ K. The corresponding spectral types of the components are B0.5IV-V and B1.5V. Line photometry produced from the disentangling solutions suggests the presence of eclipses in β Sco A, which must be verified through systematic photometry. We also present a tentative detection of possible β Cep -type line profile variability in the secondary.

Key words: stars: binaries: spectroscopic – stars: fundamental parameters – stars: individual: β Sco A

1. Introduction

Line profile variability is a phenomenon which appears to be quite common in early-type stars, and it has been well-documented by many authors. The cause of this variability is not yet understood in its entirety, but a popular and reasonably successful theory is that these variations have their origin as non-radial pulsations (NRP) in the atmospheres of these stars (cf. Ledoux 1951, Smith 1977, 1978, Walker, Yang & Fahlman 1979, 1981, Baade 1979, 1983, Vogt & Penrod 1983; for reviews, see Smith 1986, Slettebak & Snow 1987, Baade 1991 or Balona et al. 1994, among many others). We have, therefore, begun a project (SEFONO-SEarch for FOrced Nonradial Oscillations) to search for NRP in early-type binary systems in an effort to identify orbital forcing as a possible source of NRP (Harmanec et al., 1996). In this regard we mention the paper of Chapellier et al. (1995) in which the existence of a resonance phenomenon between the beat and orbital frequencies was established for 16 Lac. The implication here is that the non-radial modes in 16 Lac could be excited or enhanced by the presence of tidal effects (Kato 1974). It is therefore a likely possibility that a similar phenomenon is present in other binaries, not necessarily those with β Cep-type components, as in 16 Lac. Moreover, as the undetected secondary in 16 Lac is estimated to have a mass of only about 1 $m_{\odot}$, the resonance must be quite sensitive to the mass of the secondary star.

The binary system V436 Per, consisting of two B stars, was studied in the first paper of this series (Harmanec et al. 1996). Here, we turn our attention to the bright B-type binary β Sco A (HD 144217, HR 5984). This star has been the subject of several earlier radial velocity studies (see Table 2), and a few photometric ones as well (Stebbins 1914, Shobbrook 1978). Moreover, since the binary system has been occulted by Jupiter (Elliot et al. 1975, 1976) and the Moon (Evans et al. 1977) it is possible to derive its orbit in three dimensions, allowing reliable physical parameters to be determined. β Sco A also displays apsidal motion, with a period of about 730 years (Luyten et al. 1940). The configuration of the multiple system of which β Sco A is a part has been described in detail by Evans et al. (1977).

In this paper, we re-examine the spectroscopic orbit of β Sco A in detail, and present new radial velocities based on Reticon spectra. These data, and those already published are used to refine the orbital period and apsidal motion rate. We also examine the visual - spectroscopic orbit of the system, which has allowed us to compute a parallax and hence a distance for

Send offprint requests to: D. Holmgren

β Sco A. New physical parameters for the binary components have been derived by combining these results with those from fitting synthetic spectra to the observed line profiles. Finally, we present the results of a preliminary search for line profile variability (LPV).

2. Observations and reductions

The new spectra were obtained with the Ondřejov 2 m telescope and coudé spectrograph, used in conjunction with a Reticon detector. Twenty- six spectra covering the wavelength interval 6300Å to 6730Å at a reciprocal dispersion of 17Å mm^{-1} were obtained during 1994, 1995, and 1996. The continuum signal-to-noise ratio in a region near the He I 6678 line ranged from 160 to 1250, with a typical value of 700.

Since the entrance aperture of the image slicer of the Ondřejov spectrograph has a projected size of about three seconds of arc, light from β Sco B, which is about 0.″4 distant from A, was also collected during our observations. However, according to Evans et al. (1978), the visual magnitude of B is 5.9 ± 0.2 mag. We have therefore assumed that component B does not contribute significantly in our spectra, since the short exposure times (typically 20-30 minutes) used would mitigate against collecting a significant signal from β Sco B.

The spectra were reduced using the SPEFO program, which was specifically designed for use with Ondřejov Reticon data. This program allows for complete processing of the spectra from flat-fielding and bias subtraction through wavelength calibration and continuum rectification. The spectra were then converted to a format suitable for cross-correlation radial velocity measurement, and for use with the KOREL spectral disentangling program (Sect. 3).

All Reticon spectra had zero-point radial velocity shifts applied to them using the telluric line technique described by Horn et al. (1996).

It should be mentioned that on several nights, the observers attempted to obtain spectra closely spaced in time for the purpose of searching for line profile variability (Sect. 7). This was usually done when the components of β Sco A were close to their greatest radial velocity separation.

3. Radial velocity measurements

Radial velocities were measured for the components of β Sco A using two independent methods: cross-correlation and spectral disentangling. The latter technique has the added advantages of simultaneously producing spectroscopic elements for the binary system and a set of unblended stellar line profiles.

3.1. Cross-correlation

The cross-correlation measurements were carried out using two computer programs developed by one of us (DH). The methodology follows that described in the review paper by Hill (1993) and is thus similar to the VCROSS program. The first program, CCF3, computes the cross-correlation function (ccf) from rectified spectra linearised in logarithmic wavelength. To obtain the optimum form for the ccf, the stellar spectra are processed by CCF3 in such a way that there are no discontinuities in the data; cosine bell window functions applied to the continuum-subtracted spectra over the wavelength regions selected for inclusion in the ccf measurements are used to achieve this. Once this transformation has been applied to the template and binary star spectra, the ccf is computed using the fast Fourier transform. The resulting ccf is then used as input for a second program, CCFIT2, which fits line profile functions and a linear background to the blended ccf peaks. This program allows for the possibility of fixing any of the input parameters, which are the background level and slope, and the positions (i.e., radial velocities), widths, and heights of the ccf peaks. This feature is important for deriving a consistent set of radial velocities free from the effects of line blending.

In the case of β Sco A, a spectrum of ζ Cas (B2IV, HR 153, HD 21566, $v \sin i$ = 18 km s^{-1}) was used as the template for all ccf measurements. The radial velocity of this star was found to be 1.8 km s^{-1}, again taking a zero-point shift from telluric line measurements into account. The wavelength region 6630-6730 Å was used for the measurements, which included the O II 6641, He I 6678 and O II 6721 lines. The Hα line was not used since its inclusion would broaden the ccf peak to the extent that the blended peaks would be impossible to measure for radial velocity. The blended ccf peaks were measured for radial velocity using the "standard profile" technique (e.g., Hill and Holmgren 1995) in which a ccf of a spectrum taken near conjunction (file number 8034) is used as a non-analytic fitting function. From preliminary measurements of well-separated ccf peaks, reliable mean full-widths at half-maximum (FWHMs hereafter) of each component's ccf peak were obtained (primary: 108.0±0.5 km s^{-1}, secondary: 151±4 km s^{-1}). A second set of measurements of all blended ccfs was done in which the secondary's FWHM was held fixed at a value of 151 km s^{-1} to provide a consistent set of radial velocities. Such a step is necessary to select the physically meaningful fit from an infinite number of possible solutions. In all cases, the FWHM of the primary peak was within the error of the mean value determined earlier. These radial velocity measurements are summarised in Table 1. A typical ccf of β Sco A is shown in Fig. 1.

3.2. Disentangling

The technique of spectral disentangling was also used to provide an independent set of radial velocities, an orbit, and individual unblended line profiles for the components of β Sco A. The KOREL program of Hadrava (1995) was used for this purpose, with solutions being computed for two wavelength regions, the first for the He I 6678 line and the other spanning the Hα line. Due to the telluric line features present in the latter region, it was also necessary to converge a set of scaling factors (for each exposure) and radial velocities for these lines while solving for the binary's radial velocities, spectroscopic elements, and component profiles. The telluric lines are thus treated as a "third

Table 1. Radial velocities of β Sco A

		Cross-correlation		KOREL He I 6678		KOREL Hα	
HJD	Phase (periastron)	$V_{\rm pri}$ (km s^{-1})	$V_{\rm sec}$ (km s^{-1})	$V_{\rm pri}$ (km s^{-1})	$V_{\rm sec}$ (km s^{-1})	$V_{\rm pri}$ (km s^{-1})	$V_{\rm sec}$ (km s^{-1})
49503.5518	0.2613	−106.8	161.2	−110.03	146.89	−110.49	143.03
49784.6481	0.4290	−64.0	115.0	−75.56	111.69	−76.45	100.15
49784.6628	0.4311	−64.5	106.5	−74.38	98.17	−75.32	100.89
49787.6603	0.8701	148.7	−192.3	140.99	−197.81	146.27	−192.22
49810.5814	0.2270	−97.8	161.2	−108.25	147.88	−108.77	143.88
49810.6424	0.2360	−98.6	172.4	−107.58	159.67	−109.45	144.77
49810.6583	0.2383	−97.8	171.2	−108.48	153.27	−109.46	146.11
49829.5177	0.0003	98.5	−114.5	93.68	−123.02	92.60	−124.89
49829.5564	0.0060	91.1	−101.9	85.51	−113.69	87.48	−115.45
49829.5714	0.0082	90.2	−87.8	84.49	−107.45	81.70	−106.66
49829.6161	0.0147	82.3	−69.7	74.60	−98.92	72.45	−105.82
49830.5065	0.1451	−68.8	105.2	−78.41	97.82	−76.82	98.66
49830.5219	0.1474	−70.2	121.8	−82.18	101.86	−84.12	108.29
49830.6097	0.1603	−76.1	127.9	−87.41	107.91	−89.26	111.30
49831.5277	0.2947	−104.1	156.9	−108.04	153.00	−107.80	145.71
49831.5500	0.2980	−101.3	163.7	−107.27	152.95	−107.42	145.20
49840.5020	0.6090	7.0	7.0	−.49	15.81	−3.77	8.56
49840.5263	0.6126	7.9	7.9	−.40	2.62	.65	−.97
49843.4911	0.0468	30.7	−4.2	27.45	−36.74	24.01	−35.06
49861.4452	0.6762	34.9	−3.2	31.10	−35.66	29.75	−34.58
49863.4647	0.9720	130.9	−164.1	121.87	−174.58	125.15	−170.48
49863.5396	0.9830	120.7	−147.3	113.63	−159.27	117.13	−153.48
50162.6099	0.7831	101.0	−124.5	97.69	−135.10	100.91	−125.92
50162.6199	0.7845	103.0	−120.0	98.96	−131.02	95.81	−125.96
50162.6417	0.7877	102.0	−128.5	100.14	−141.75	97.85	−128.64
50163.6453	0.9347	141.0	−205.0	144.11	−199.98	141.62	−187.13

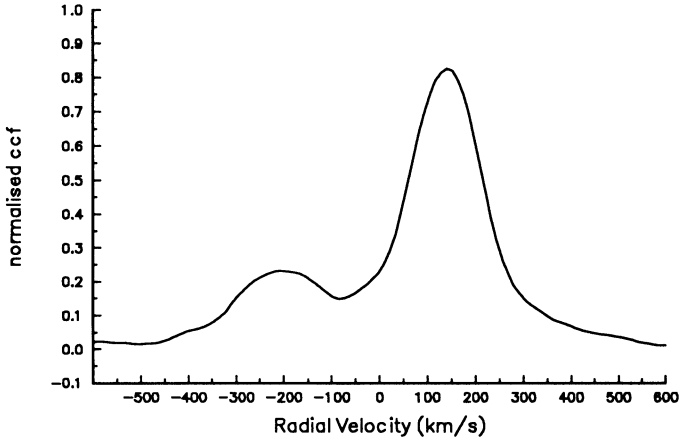

Fig. 1. A cross-correlation function (ccf) for β Sco A near orbital phase 0.9 , close to the maximum radial velocity separation

component". The disentangling solution for Hα therefore proceeded in two steps; the first to converge the telluric line parameters and the second to converge the binary parameters. The binary orbital elements found from the He I 6678 solution were used as starting values for the Hα solution. The radial velocities produced by KOREL are summarised in Table 1, while the orbital elements are given in columns 3 and 4 of Table 3. The orbital period was held fixed at $6\overset{\rm d}{.}828245$ (Sect. 4) in the solutions for both wavelength regions. All other orbital parameters of the binary were allowed to vary. We note here that apsidal motion is not taken into account in the KOREL solutions, but over the time interval during which the Reticon data were obtained, the change in the longitude of periastron is negligible. The reconstructed component line profiles are shown in Figs. 2 and 3, and the radial velocities for both wavelength regions are shown in Fig. 4. It should be stressed here that KOREL cannot determine a systemic velocity, so all of its radial velocities will be shifted accordingly. Moreover, the reconstructed stellar line profiles both have zero mean value, but have been shifted arbitrarily in Figs. 2 and 3. The present version of KOREL is unable to produce realistic errors in the orbital elements on account of the complexity of the spectral disentangling problem, but the interagreement of the two KOREL solutions and their agreement with the cross-correlation results illustrates the uncertainties in the disentangling solutions. We now turn to a discussion of the other spectroscopic orbits.

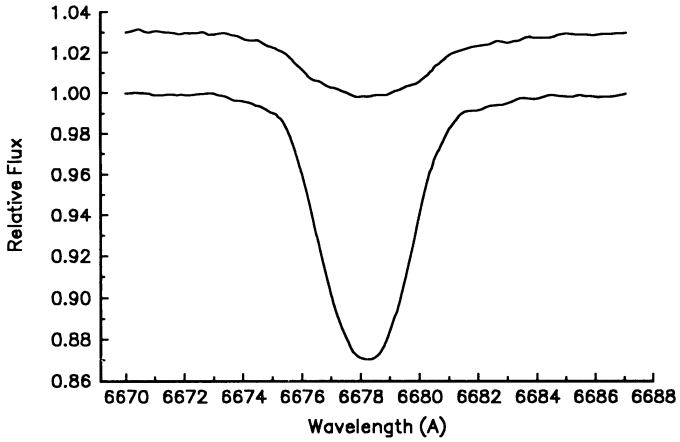

Fig. 2. Component He I 6678 Å line profiles recovered by KOREL. The secondary profile (top) has been shifted upward for clarity

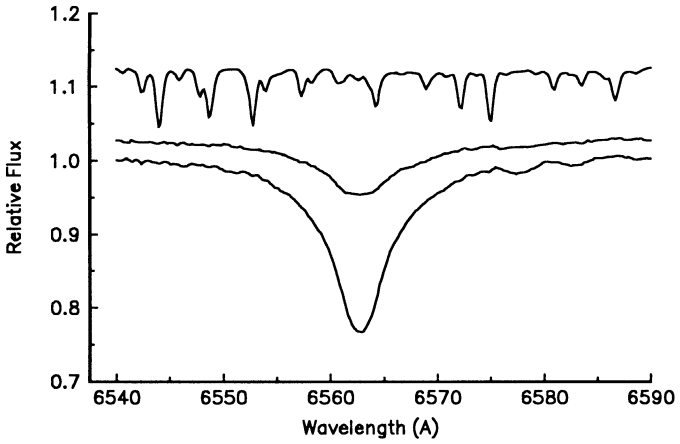

Fig. 3. Component Hα line profiles and telluric line spectrum recovered by KOREL. The secondary's profile and telluric spectrum have been shifted upward for clarity

4. Orbital analyses

Given the nature of the data available to us, it has been necessary to use three different approaches for determining the orbit of β Sco A. We have analysed all available published radial velocity data, and our new data measured using the cross-correlation and disentangling techniques. It has also been possible to determine an orbit in three dimensions (a visual - spectroscopic orbit) using published position angles and separations from occultations of the system by Jupiter and the Moon. These different sources of data have allowed us to determine reliable absolute dimensions, and to refine the orbital period and apsidal motion rate. As the disentangling (KOREL) results have been discussed in some detail already, we proceed on to the other solutions.

4.1. Spectroscopic orbits

All previously published radial velocities available in Ondřejov were used in conjunction with the new data to refine the orbital period and apsidal motion rate. A number of previously published radial velocity data sets have been used, and the details of these various data sets are summarised in Table 2. A total of 603 radial velocities were used in the combined solutions discussed below (Fig. 6). The few observations published by Slipher (1903) were not used on account of the fact that the observation times are not known precisely. The GMT and UT dates used in the Allegheny (Daniel and Schlesinger, 1912) and Lick (Abhyankar, 1959) data were converted to heliocentric Julian dates, and the geocentric Julian dates used in the Lowell (Duncan, 1912) data converted to heliocentric values.

Table 2. Radial Velocity Data Sets

Source	Weight		Dispersion	Wavelength
	Primary	Secondary	(Å mm^{-1})	(Å)
1	2.147	0.360	17	6300-6750
2	2.022	0.272	11.2	3900-4800
3	2.111	0.091	10	4300-4750
4	1.380	0.157	-	4000-4500
5	1.487	0.320	30,60	-
6	1.541	0.113	-	4000-4500

References for datasets: 1. Present paper. 2. Peterson et al. (1979). 3. Abhyankar (1959). 4. Daniel and Schlesinger (1912). 5. Luyten et al. (1940). 6. Duncan (1912).

For the purpose of computing a combined solution of all available radial velocities, the FOTEL program of Hadrava (1990) was used since it allows the user to solve for the zero-point (i.e., systemic velocity) of each data set and the apsidal motion rate, in addition to the usual set of orbital elements (which are determined using all datasets). Moreover, FOTEL produces a rms scatter about the fit for each data set. We have, therefore, assumed that any instrumental differences between data sets manifest themselves purely as zero-point shifts. Since the different radial velocity data sets were taken with different instruments, it is necessary to weight each source of data correctly. We have adopted the following approach, similar to that used by Holmgren et al. (1995) in their analysis of the times of minima of Y Cyg. Spectroscopic orbits were computed using FOTEL for each data set separately. Relative weights for each data set were then taken to be inversely proportional to the mean-square residuals from each solution, and a combined solution computed using these weights (Table 3, column 5). In this solution, all orbital elements including the period and apsidal motion rate were varied. In addition, each set of primary and secondary radial velocities was assigned its own systemic velocity and relative weight. In total, 12 data sets were used in this solution. This approach was adopted, since - particularly for the older data sets - the quality of the secondary's radial velocities was obviously much poorer than that of the primary's velocities. With this solution we have verified that the apsidal motion rate is 0.00131 ± 0.00004 degrees per day, and have refined the orbital period (Table 3, column 5). As an independent check on the apsidal motion rate we have used the values of ω published by the different authors, which are conveniently summarised in

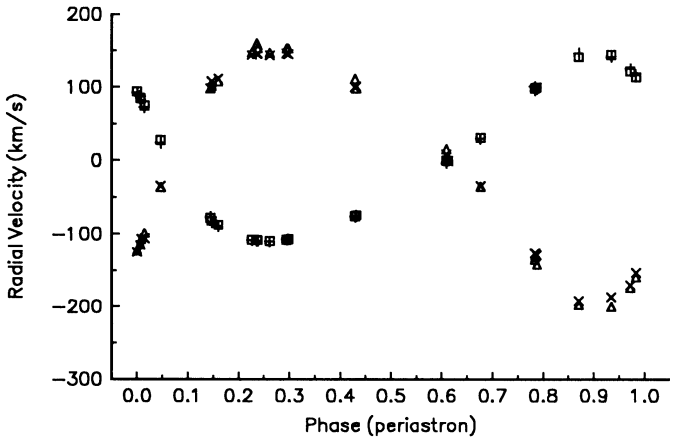

Fig. 4. KOREL radial velocities from the He I 6678 Å and Hα lines. Open symbols denote helium data, crosses denote hydrogen data

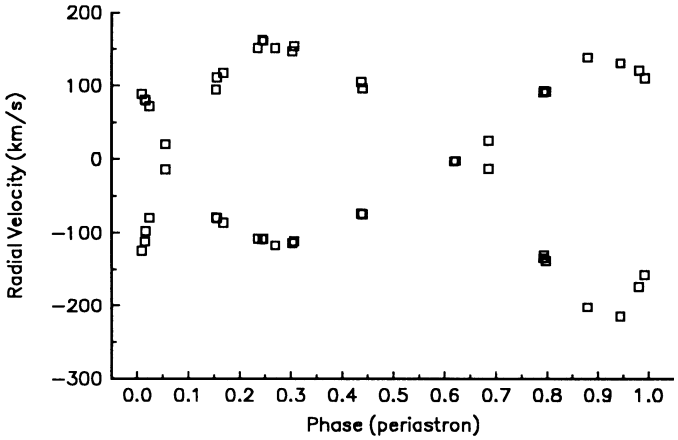

Fig. 5. Cross-correlation radial velocities for β Sco A

the work of Peterson et al. (1979). A linear least-squares fit to all available values of ω was used to compute an apsidal motion rate of 0.00119 ± 0.00015 degrees per day, which is in good agreement with the value found by FOTEL. The apsidal period corresponding to the rate found by FOTEL is 752 ± 52 years. Unless stated otherwise, errors in all quantities used throughout this paper refer to one standard deviation (i.e., $\pm\sigma$).

We have also used FOTEL to compute a solution for the Reticon data (cross-correlation radial velocities) alone, (Fig. 5) which is given in column 2 of Table 3. This solution does take into account the apsidal motion rate, although this parameter was held constant for this particular fit. Given that the older data sets produce lower primary and larger secondary semi-amplitudes, presumably due to the more subjective nature of the measurements, we have adopted the orbits based on the Reticon data (either ccf or KOREL results) as those from which the absolute dimensions are to be computed. The period and apsidal motion rate used in these orbits are those determined using all of the data sets.

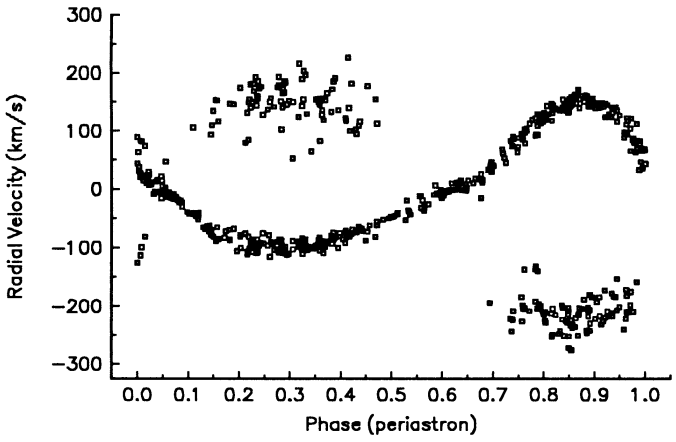

Fig. 6. All available radial velocities for β Sco A

4.2. The orbit of the visual companion

From the combined solution discussed in Sect. 4.1, it is apparent that the systemic velocity of β Sco A has changed significantly since the first radial velocity observations were obtained. It is, therefore, possible that this variation could be due to the orbital motion of the AB pair. To examine this possibility further, a joint solution of all primary star data was computed with FOTEL (see the last column of Table 3). We have included only the primary's velocities here since those of the secondary are, with the exception of the new data, of a much lower quality. The errors of the various systemic velocities shown in Fig. 7 are those from the joint least-squares solution and thus do not reflect the real (and unknown) errors in the individual radial velocities. Hence, the sizes of these error bars reflect the scatter in the individual data sets. A plot of the various systemic velocities from the joint solution with respect to their epochs gives a linear trend which could be due to the relative motion of the AB pair (Fig. 7). In this interpretation, assuming a circular orbit, the slope of the line specifies $2\pi K_3/P$ where K_3 and P refer to the motion of B about A, and at present it is not possible to separate these two quantities. We note here that the value of the slope is $(5.6 \pm 1.1) \times 10^{-4}$ km s^{-1} day^{-1}. Further visual and spectroscopic data on the AB pair will be required to resolve this matter.

4.3. The visual - spectroscopic orbit

The components of β Sco A were resolved during occultations by Jupiter (Elliot et al., 1975) and the Moon (Evans et al., 1977), thus providing two measurements of relative separation (ρ) and position angle (θ). These measurements and the radial velocity difference data have allowed us to solve for the orbital elements in three dimensions. Additional constraints on the orbital inclination are provided by the angular radii (Elliot et al., 1976), and apparent absence of eclipses (Stebbins, 1914). Both of these indicate that the orbital inclination must be less than 70°. This constraint should also be checked observationally with new photometric data.

Table 3. Spectroscopic orbits of β Sco A

Parameter*	ccf	KOREL (Hα)	KOREL (He I 6678)	All data	All primary
γ_{1P} (km s^{-1})	10 ± 1	-	-	8.7 ± 1.1	9.2 ± 1.1
γ_{2P} (km s^{-1})	-	-	-	-1.9 ± 1.3	-2.0 ± 1.2
γ_{3P} (km s^{-1})	-	-	-	-0.3 ± 0.7	-0.5 ± 0.7
γ_{4P} (km s^{-1})	-	-	-	-11 ± 1	-12 ± 1
γ_{5P} (km s^{-1})	-	-	-	-5.4 ± 1.1	-5.4 ± 1.1
γ_{6P} (km s^{-1})	-	-	-	-8.5 ± 0.9	-8.6 ± 0.9
γ_{1S} (km s^{-1})	-	-	-	11 ± 4	-
γ_{2S} (km s^{-1})	-	-	-	3.6 ± 5.5	-
γ_{3S} (km s^{-1})	-	-	-	-12 ± 9	-
γ_{4S} (km s^{-1})	-	-	-	36 ± 5	-
γ_{5S} (km s^{-1})	-	-	-	6.8 ± 5.2	-
γ_{6S} (km s^{-1})	-	-	-	8.7 ± 8.8	-
K_P (km s^{-1})	130 ± 2	133	133	125.4 ± 0.6	125.5 ± 0.6
K_S (km s^{-1})	181 ± 5	175	178	201 ± 3	-
e	0.300 ± 0.010	0.309	0.285	0.276 ± 0.042	0.285 ± 0.043
ω_0 (deg)	53.6 ± 2.1	54.6	54.6	58.6 ± 1.8	58.8 ± 1.0
$\dot{\omega}$ (deg day^{-1})	$0.00131f$	-	-	0.00131 ± 0.00009	$0.00131f$
T_{peri}	49788.49 ± 0.03	49788.52	49788.52	49788.547 ± 0.028	49788.553 ± 0.016
P_a (days)	$6.828245f$	$6.828245f$	$6.828245f$	6.828245 ± 0.000009	$6.828245f$
P_s (days)	$6.828076f$	-	-	6.828076	6.828076
$\pm\sigma_1$ (km s^{-1})	7.8	6.5	5.9	21	8.6

Notes: * P,S refer to primary and secondary components. $P_{a,s}$: Subscripts a, s refer to anomalistic and sidereal periods. σ_1 : Standard error of a single observation of unit or average weight. f : Denotes that parameter was fixed during solution.

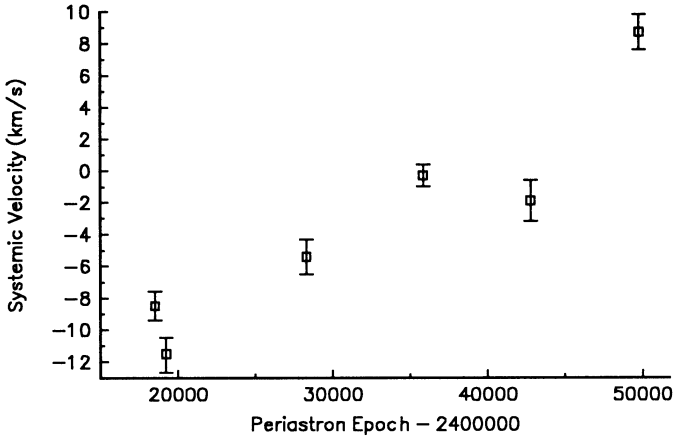

Fig. 7. Systemic radial velocities for the primary of β Sco A

The combination of visual and spectroscopic data into a joint least-squares solution with constraints on any of the orbital elements is discussed by Morbey (1975). A modification of the Levenberg-Marquardt gradient expansion method for constrained least-squares problems was presented by Jeffreys (1981). We refer the reader to the papers by Morbey and Jeffreys for further details. One of us (DH) has created a computer program to calculate a visual - spectroscopic orbit. The use of such a method is necessary when combining different kinds of data into one solution to obtain realistic errors for the elements and the parallax. It also allows us to incorporate the fact that we know the period very accurately, and thus to employ this knowledge as a constraint on the solution. The elements solved for were a, the semi-major axis, the orbital inclination i, the eccentricity e, the sum of the semiamplitudes $K_p + K_s$, the longitude of periastron ω, the position angle of the line of nodes Ω, and the time of periastron passage T. The period was constrained to have the value of $6^d.828245$. The cross-correlation radial velocities were used to form the radial velocity difference data for this solution, which is summarised in Table 4. Following Morbey, the radial velocities, position angles, and separations were weighted according to the inverse squares of their errors, with the solution being obtained by minimizing the sum (over all available data) of squares

$$\chi^2 = \sum \left[\left(\frac{\Delta V}{\sigma_v} \right)^2 + \left(\frac{\Delta \rho}{\sigma_\rho} \right)^2 + \left(\frac{\Delta \theta}{\sigma_\theta} \right)^2 \right]$$

where $\sigma_v, \sigma_\rho, \sigma_\theta$ are the errors in the radial velocity difference, separation, and position angle data respectively, and ΔV, $\Delta \rho$, and $\Delta \theta$ are their respective fit residuals. Errors in the position angles and separations have been published, but for the radial velocity difference data we have assumed an error of ± 6 km s^{-1}, based on the rms scatter σ_1 from the orbital solution of the cross-correlation radial velocities (cf. Table 3). The most important result which follows from the solution is the value of the semi-major axis a , which has allowed the parallax (denoted here as

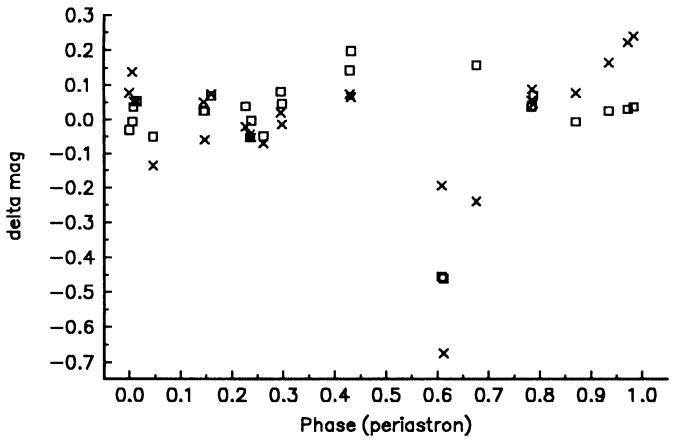

Fig. 8. Line photometry of β Sco A. Squares denote results from He I 6678 Å and crosses those from Hα

Table 4. Visual - spectroscopic orbit for β Sco A

Parameter	
a (arcsec)	1.42 ± 0.02
$K_{\rm pri} + K_{\rm sec}$ (km s^{-1})	309 ± 2
e	0.291 ± 0.006
i (degrees)	111.8 ± 0.7
ω (degrees)	54.8 ± 1.3
Ω (degrees)	294.2 ± 0.8
$T_{\rm peri} - 2400000$	49788.509 ± 0.019
P (days)	6.828245 (fixed)
$(a_1 + a_2) \sin i$ (R$_\odot$)	39.9 ± 0.3
$(a_1 + a_2)$ (R$_\odot$)	43.0 ± 0.4
$(m_1 + m_2) \sin^3 i$ (M$_\odot$)	18.4 ± 0.4
$(m_1 + m_2)$ (M$_\odot$)	22.9 ± 0.6

π) for β Sco A to be determined. Together with the inclination, the parallax has allowed us to determine the absolute dimensions and distance to the system. It should be mentioned here that the inclination angle found from the visual - spectroscopic solution follows the convention for this parameter for visual binary systems. Thus, an inclination angle of 111.8 degrees can be seen to be *equivalent* to an inclination of 68.2 degrees in the case of an eclipsing or spectroscopic system.

The visual - spectroscopic solution shows good agreement with the spectroscopic solution of the ccf data (Table 3).

4.4. An alternative route to the orbital inclination

A limit on the orbital inclination may also be derived independently of the occultation measurements, and hence provide a check on the physical parameters of β Sco A. We employ here a method similar to that used by Holmgren et al. (1990) with NY Cep. From the corrected Moon-Dworetsky calibration (Sect. 5.2), the observed four-colour data and light ratio, we have estimates of $M_{\rm V}$ for both components, and these provide estimates of the effective temperatures as well if one uses the calibration of Popper (1980). For the primary and secondary respectively, this gives 28500 K and 26500 K. In turn, $M_{\rm bol}$ for each component gives its radius. From these radii and the spectroscopic orbit based on the Reticon data alone, a limit on the inclination for which eclipses can occur can be set using (Scarfe, 1979)

$$\frac{(R_1 + R_2)(1 + e\cos v)}{a \sin i (1 - e^2)} \leq \cot i$$

where $v \simeq \pi/2 - \omega$ refers to the true anomaly at the primary eclipse, which is assumed to be absent in the case of β Sco A . The limit on the inclination from this relation is then $i \leq 71.7$ degrees. Given the assumptions made in this calculation, it is clear that this result is consistent with the inclination derived from the visual - spectroscopic solution.

5. Basic physical parameters

5.1. Masses, parallax, and radii

The masses of the components of β Sco A may be determined using the minimum masses from the spectroscopic orbit and the inclination from the visual - spectroscopic orbit. In this way, we find the masses shown in Table 5. The errors in the masses take into account all significant sources of uncertainty.

We have calculated a parallax for β Sco A using the results from the visual - spectroscopic orbit. By combining the spectroscopic value of $(a_1 + a_2) \sin i$ with the semi-major axis of the visual orbit, we find that $\pi = 0\farcs0070 \pm 0\farcs0001$. The corresponding distance is 143 ± 3 pc. The errors in the parallax and distance are probably optimistic, since sources of unknown systematic errors have not been taken into account. The distance is in reasonable agreement with the 186 pc found for Upper Scorpius by de Geus et al. (1989) from their analysis of Walraven photometry, when one takes into account a mean $\pm 0\fm3$ uncertainty in their values of $M_{\rm V}$ and corrects for the magnitude difference between the components.

The absolute radii of the components are determined by combining the angular radii (Elliot et al., 1976) and the parallax, and they are presented in Table 5. We have adopted the published errors in the angular radii to compute the errors in the absolute ones.

The absolute dimensions and radiative parameters ($M_{\rm V}$, $T_{\rm eff}$, $\log g$, and spectral type) for β Sco A are summarised together in Table 5. Using the mean relations of Harmanec (1988), the components of β Sco A have the correct masses and radii for their spectral types.

5.2. Radiative parameters

The published MK classifications for β Sco A are B1V (Abt, 1981), B0.5V (Garrison et al., 1977), and B0.5V (Slettebak, 1968). From fits of synthetic spectra, we have adopted a spectral type of the primary of B0.5V.

Table 5. β Sco A-physical parameters using inclination from visual - spectroscopic orbit

Parameter	Primary	Secondary
$m \sin^3 i$ ($M_\odot$)	10.8 ± 0.7	7.7 ± 0.3
$a \sin i$ ($R_\odot$)	16.7 ± 0.3	23.3 ± 0.6
m ($M_\odot$)	13.3 ± 0.9	9.5 ± 0.4
r ($R_\odot$)	6.5 ± 0.4	4.0 ± 0.3
$T_{\rm eff}$ (K)	28000 ± 2000	24600 ± 2000
$\log g$ (cgs)	3.95 ± 0.33	4.20 ± 0.35
$M_{\rm V}$ (mag)	-3.38 ± 0.23	-2.06 ± 0.23
Spectral type	B0.5IV-V	B1.5V

Table 6. β Sco A-photometric colors and reddening

Parameter[a]	Observed[b]	Intrinsic	Primary[c]	Secondary[c]
V	2.63	2.12	2.40	3.72
$b-y$	0.006	-0.113	-0.118	-0.100
$E(b-y)$	0.119	-	0.122	0.116
m_1	0.046	0.085	0.074	0.090
c_1	0.013	-0.010	-0.047	0.129
$u-b$	0.117	-0.064	-0.134	0.110
$[u-b]$	-	0.108	0.046	0.263
β	2.614	-	2.604	2.633

Notes: [a] All data are in magnitudes. [b] Primary and secondary combined. [c] Intrinsic colors.

To obtain preliminary estimates of the effective temperatures and logarithmic surface gravities of the components, we have used the published Strömgren photometry of Hauck and Mermilliod (1990) and Shobbrook (1978). The intrinsic colors, reddening, component temperatures and logarithmic surface gravities have been determined using the calibrations of Balona (1984), and Moon and Dworetsky (1985), as corrected by Napiwotzki et al. (1993). The photometric data are summarised in Table 6. As Shobbrook has published colors for the primary star, we have an independent check on our results. Both calibrations give an effective temperature of 28000 K for the primary, and 21000 K for the secondary. The surface gravities are $\log g$ = 3.91 and 4.17 [CGS] for the primary and secondary respectively. The values for the primary star correspond to a spectral type of B0.5IV-V. By assuming that $\Delta V = \Delta M_{\rm V}$, and using the known magnitude difference the implied spectral type of the secondary is B1.5V, if the calibrations of Crawford (1978) are used. On the scale of Popper (1980), this corresponds to $T_{\rm eff}$ = 26400 K. Our fits of synthetic spectra favour this latter temperature for the secondary. From combined Walraven colors, de Geus et al. (1989) find $T_{\rm eff}$ = (26300$\pm$2000) K and $\log g$ = 3.78 $\pm$ 0.25 for β Sco A, in agreement with the results described here. We note that the secondary's spectral type places it in the β Cep instability strip.

Synthetic spectra for our analysis were calculated from the Kurucz (1993b) grid of solar composition LTE line blanketed model atmospheres using the computer code SYNSPEC (for a description see Hubeny et al. 1994). Line data were taken from the list of Kurucz (1993a).

The fact that we used LTE plane parallel model atmospheres does not mean that both assumptions are valid throughout the line forming region. There are several reasons that support this simplification. First, our analysis is based on a very limited wavelength range. Any fit to the observed spectrum is charged by quite a large uncertainty regardless the sophistication of the adopted model atmosphere. Thus, calculations of complicated model atmospheres only for this purpose is just wasting computer time and memory and using LTE model atmospheres is suitable for present purposes. In addition, the fact that models are line blanketed pushes the adopted models towards reality. Second, the sphericity effects on lines are pronounced especially for lines forming in outer regions, as e.g. Hα (Kubát 1996). Lines forming in continuum forming regions are affected only marginally, if at all.

Knowing the light ratio, temperatures and logarithmic surface gravities of the components of β Sco A has allowed us to fit synthetic spectra and hence determine the projected rotational velocity $v \sin i$ for each component. Both the original spectra and the component profiles recovered by KOREL have been used. Due to the limited grid of models available (the steps are 1000K in $T_{\rm eff}$ and 0.5 in $\log g$) we adopted for the synthetic spectrum the following values of effective temperature and surface gravity: $T_{\rm eff}$ = 28000 K, $\log g$ = 4.0, and $T_{\rm eff}$ = 26000 K, $\log g$ = 4.0 for the primary and secondary, respectively.

It is also possible to use the strength of the O II 6721Å line as a temperature indicator, and we have found that our adopted effective temperature for the secondary of β Sco A gives a better fit to this line than a model with a cooler temperature.

The adopted radiative parameters are presented in Table 5.

5.3. Light ratio and projected rotation velocity

An estimate of the light ratio, independent of the absolute dimensions, was determined from the relative fluxes in the He I 6678 line for both components. These were measured from 8 Reticon spectra on which the components were well-separated. Petrie's (1939) method was used since the component line profiles are blended even at the maximum radial velocity separation. The light ratio was thus found to be $l(p/s) = 4.073 \pm 0.050$ which corresponds to a magnitude difference of $1\overset{\rm m}{.}525 \pm 0\overset{\rm m}{.}014$ at 6678 Å. A similar measurement using equivalent widths was attempted, but the results were too sensitive to the placement of the continuum level to be of any use. The line photometry results from KOREL (Sect. 6) indicate light ratios of 3.2 and 3.5 for Hα and He I 6678, respectively, which are in broad agreement with the results from Petrie's method. A visual magnitude difference of $1\overset{\rm m}{.}3$ (or a light ratio of 3.51) for β Sco A has been published by Shobbrook (1978). We have adopted a light ratio of 3.5, which is in agreement with the difference in absolute magnitudes computed from the absolute dimensions.

From the fits of the synthetic spectra to the component line profiles we find $v \sin i$ to be 90 km s^{-1} and 135 km s^{-1} for

the primary and secondary, respectively. These values take into account the width of the instrumental profile, which was estimated to be 32 km s^{-1} from the widths of unblended telluric (water vapour) lines. The errors in the projected rotational velocities are less than $\pm$5km s^{-1}. It is clear from the projected rotation velocities that the primary star rotates synchronously at periastron while the secondary rotates 2.4 times faster than this.

5.4. Internal structure constant

With the absolute dimensions, projected rotational velocities, and apsidal motion rate determined, a mean internal structure constant (ISC hereafter) can be computed for β Sco A and compared with the recent model computations of Claret and Giménez (1992).

Following the usual procedure (e.g., Claret and Giménez 1993), we find a mean ISC of $\log \bar{k}_{2,\mathrm{obs}} = -1.98 \pm 0.14$. This value takes into account a correction for the relativistic apsidal motion rate, and also for the fact that only the primary component of β Sco A rotates with the orbital rate at periastron. The mean observed ISC compares favourably with a theoretical value of -2.06. To compute the latter, we have used Tabs. 18 and 19 of Claret and Giménez (1992) which assume a composition $(Y, Z) = (0.280, 0.02)$. From the $\log T_{\mathrm{eff}} - \log g$ diagram (Fig. 4) of the same paper, the ages of the component stars are approximately 10^7 yrs. Moreover, the observed masses and those estimated from the $\log T_{\mathrm{eff}} - \log g$ diagram agree to within the errors of the former. The age of β Sco A derived here is in reasonable agreement with the kinematic age (5×10^6 yrs) of Blaauw (1964, 1978) and the nuclear age ($5 - 6 \times 10^6$ yrs) derived by de Geus et al. (1989) from Walraven photometry.

6. Line photometry

The latest version of the KOREL disentangling solutions (see Hadrava 1996 for details) also generated phase-dependent flux multipliers for each exposure. These multipliers take into account any light loss due to eclipses or intrinsic variability. Moreover, it is possible to convert these multipliers to a magnitude scale and thus obtain a set of phase-dependent *magnitude differences between the primary and secondary*. It should be stressed that in no sense is this a conventional light curve (which is given as phase-dependent total magnitude of the binary) or is it flux-calibrated photometry.

The flux multipliers found by KOREL may also be used in a further nonlinear least-squares fit to determine the light ratio in each of the wavelength regions used for the disentangling solutions (see eq. 13 of Hadrava, 1996). It should be mentioned here that we do not have objective estimates of the errors in these light ratios.

Fig. 8 shows the line photometry results for β Sco A for both Hα and He I 6678. Of greatest interest here is the presence of what appears to be an eclipse near phase 0.6. From the spectroscopic orbits and known inclination for the system, FOTEL predicts that - if eclipses are present - an eclipse should occur at this phase, but also near phase 0.05 as well. However, the latter eclipse appears to be absent, or at least marginally present. We are reluctant to assign much significance to this detection of eclipses in β Sco A until systematic, calibrated photometry is obtained. It is true, however, that the same technique has detected an eclipse of V436 Per at correct orbital phase (cf. Harmanec et al. 1996).

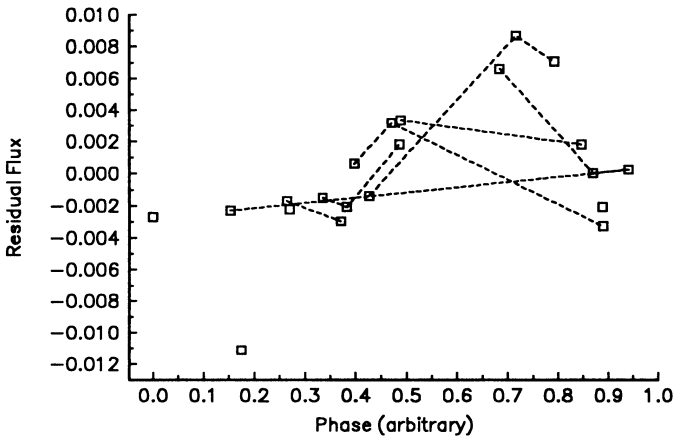

Fig. 9. Phase plot (period = $0^{\mathrm{d}}.17333$) of residual fluxes from difference spectra of β Sco A. Squares denote data points and the lines connect exposures obtained on the same night. The long line connects two exposures with long exposure times

7. Search for line profile variability

From the results of Sect. 5, it can be seen that the secondary of β Sco A falls into the correct range of spectral types for β Cep stars. In fact, Shobbrook (1978) observed β Sco A for this very reason, but was apparently unable to detect any light variation. We have therefore examined the He I 6678 line profiles for any indications that line profile variability (LPV hereafter) might be present. For this purpose we have used both difference spectra and the line photometry results of the previous section.

The difference spectra were generated in two steps. First, a spectrum taken near conjunction (file 8034) was lightly smoothed. The resulting spectrum was then shifted and scaled to match the primary's line profile on each exposure and then subtracted. One of these difference spectra was then lightly smoothed and the process repeated to remove the secondary's line profile.

The residual flux at 6678.151 Å was measured on each difference spectrum and the resulting time series subjected to a periodogram analysis (Horne and Baliunas, 1986, Scargle, 1982). A linear trend was removed from the residual fluxes before the periodogram was computed, and a sampling interval of 10^{-4} cycles per day used for the periodogram calculation. A significant peak (false alarm probability of 0.0383) was found at a frequency of 5.7692 c d^{-1}. This frequency corresponds to a period of about $0^{\mathrm{d}}.17$. We note here that due to the relatively high frequency of this signal, and the presence of its 1d aliases, the false alarm probability stated above is purely formal. Moreover,

the number of independent frequencies adopted for the calculation of this probability is $N_i = 19.1$, according to equation (13) of Horne and Baliunas.

Difference spectra were also generated using an alternative technique, based on the He I 6678 line profiles recovered by KOREL. For each observed spectrum, the profiles from KOREL were shifted to the positions of the primary and secondary components, scaled according to the light ratio, and then subtracted from the observed spectrum. An examination of the resulting difference spectra did not reveal any travelling "bumps" characteristic of NRP.

The line photometry data were also subjected to periodogram analyses, with the He I 6678 Å and Hα data producing a significant signal at 1.5253 c d^{-1} (false alarm probability of 0.011, $N_i = 20.4$) and 5.8730 c d^{-1} (false alarm probability of 0.0075, $N_i = 21.6$), respectively. However, given that the uncertainty in these measures is about $\pm 0\overset{\mathrm{m}}{.}05$, these detections should be viewed with some skepticism.

If one adopts the period detected from the difference spectra and plots the data in a phase diagram (Fig. 9), then a plausible variation is produced. If this variation is real, it could correspond to the β Cep-type variation of the secondary. However, this result should be viewed with some caution until it can be checked using data with a much higher resolution (both spectral and temporal) and signal-to-noise.

8. Summary

New spectroscopic data are presented which we have used together with various sources of published data to derive new, more precise physical parameters of β Sco A. For the primary and secondary respectively, we find: $m_{\rm p}/m_{\odot} = 13.5 \pm 0.9$, $m_{\rm s}/m_{\odot} = 9.6 \pm 0.4$, $r_{\rm p}/r_{\odot} = 6.8 \pm 0.4$, $r_{\rm s}/r_{\odot} = 4.2 \pm 0.3$, $T_{\rm p} = 28000 \pm 2000$ K, and $T_{\rm s} = 26400 \pm 2000$ K. These results have also led to an improved parallax ($0\overset{''}{.}0070 \pm 0\overset{''}{.}0001$) and distance ($143 \pm 3$ pc) to the system. Photometry generated from the He I 6678 Å and Hα line profiles suggests the presence of eclipses. A preliminary search for line profile variability has resulted in the tentative detection of a period of $0\overset{\mathrm{d}}{.}17333$ in the residual flux from the secondary star, which is proposed to be a β Cep-type star.

Acknowledgements. The authors would like to thank an anonymous referee for comments on an earlier version of the paper. DH would like to thank Dr. S. Štefl for an illuminating discussion on the detection of line profile variability, Mrs. A. Kalašová for entering some of the radial velocity data, and Dr. G. Scholz of the Astrophysikalische Institut Potsdam for obtaining the papers by Slipher, Duncan, and Luyten et al., which were not available at Ondřejov. The use of the computerized bibliography from the Strasbourg Astronomical Data Centre is gratefully acknowledged. We would also like to thank V. Šimon and P. Škoda for obtaining some spectra of β Sco A used in this study. This study was supported by the grant 205/96/0162 of the Grant Agency of the Czech Republic and also by the project K1-003-601/4 *Astrophysics of non-stationary stars* of the Academy of Sciences of the Czech Republic.

References

Abhyankar K.D. 1959, ApJS 4, 157
Abt H.A. 1981, ApJS 45, 437
Baade D. 1979, thesis, Astron. Inst. Univ. Münster
Baade D. 1983, Hvar Obs. Bull. 7, 185
Baade D. (Ed.) 1991, in Rapid Variability of OB-Stars: Nature and Diagnostic Value, ESO Conf. Proc. No. 36, ESO, Garching
Balona L.A. 1984, MNRAS 211, 973
Balona L.A., Henrichs H.F., Le Contel J.M. (Eds.) 1994, in Pulsation, Rotation and Mass Loss in Early-Type Stars, IAU Symp. 162, Kluwer, Dordrecht
Blaauw A. 1964, ARA&A 2, 213
Blaauw A. 1978, in Problems of Physics and Evolution of the Universe, ed. L. Mirzoyan, Yerevan, USSR, 101
Chapellier E., Le Contel J.M., Le Contel D., Sareyan J.P., Valtier J.C. 1995, A&A 304, 406
Claret A., Gimenéz A. 1992, A&AS 96, 255
Claret A., Gimenéz A. 1993, A&A 277, 487
Crawford D.L. 1978, AJ 83, 48
Daniel Z., Schlesinger F. 1912, Pub. Allegheny Obs. 2, 127
de Geus E.J., de Zeeuw P.T., Lub J. 1989, A&A 216, 44
Duncan J.C. 1912, Lowell Obs. Bull. no. 54, 21
Elliot J.L., Rages K., Veverka J. 1975, ApJ 197, L123
Elliot J.L., Rages K., Veverka J. 1976, ApJ 207, 994
Evans D.S., Elliot J.L., Peterson D.M. 1978, AJ 83, 438
Evans D.S., Africano J.L., Fekel F.C., Montemayor T., Palm C., Silverberg E., Van Citters W., Wiant J. 1977, AJ 82, 495
Garrison R.F., Hiltner W.A., Schild R.E. 1977, ApJS 35, 111
Hadrava P. 1990, Contr. Astron. Obs. Skalnaté Pleso 20, 23
Hadrava P. 1995, A&AS 114, 393
Hadrava P. 1996, A&AS (in press)
Harmanec P. 1988, Bull. Astron.Inst.Czechosl. 39, 329
Harmanec P., Hadrava P., Yang S., Holmgren D., North P., Koubský P., Kubát J., Poretti E. 1996, A&A (in press)
Hauck B., Mermilliod M. 1990, A&AS 86, 107
Hill G. 1993, in New Frontiers in Binary Star Research, K.-C. Leung and I.S. Nha (eds.), Astronomical Society of the Pacific Conference Series 38, 127
Hill G., Holmgren D.E. 1995, A&A 297, 127
Holmgren D.E., Hill G., Scarfe C.D. 1995, Observatory 115, 188
Holmgren D.E., Hill G., Fisher W., Scarfe C.D. 1990, A&A 231, 89
Horn J., Kubát J., Harmanec P., Koubský P., Hadrava P., Šimon V., Štefl S., Škoda P. 1996, A&A 309, 521
Horne J.H., Baliunas S.L. 1986, ApJ 302, 757
Hubeny I., Lanz T., Jeffery C.S. 1994, in Newsletter on Analysis of Astronomical Spectra No.20, C.S.Jeffery ed., St. Andrews University, p.30
Jeffreys W.H. 1981, AJ 86, 149
Kato S. 1974, PASJ 26, 341
Kubát J. 1996, in Model atmospheres and spectrum synthesis, S.J. Adelman, F. Kupka & W.W. Weiss eds., Astronomical Society of the Pacific Conference Series 108, in press
Kurucz R.L. 1993a, Atomic Data for Opacity Calculations, Kurucz CD-ROM No.1
Kurucz R.L. 1993b, Solar Abundance Model Atmospheres, Kurucz CD-ROM No.19
Ledoux P. 1951, ApJ 114, 373
Luyten W.J., Struve O., Morgan W.W. 1940, Yerkes Obs. Pub. 7, 264
Moon T.T., Dworetsky M.M. 1985, MNRAS 217, 305
Morbey C.L. 1975, PASP 87, 689

Napiwotzki R., Schönberner D., Wenske V. 1993, A&A 268, 653
Peterson D.M., Elliot J.L., Mink D.J. 1979, PASP 91, 87
Petrie R.M. 1939, Publ. Dominion Astrophys. Obs. 7, 205
Popper D.M. 1980, ARA&A 18, 115
Scarfe C.D. 1979, J.R.Astron.Soc.Can. 73, 258
Scargle J.D. 1982, ApJ 263, 835
Shobbrook R.R. 1978, MNRAS 184, 43
Slettebak A. 1968, ApJ 151, 1043
Slettebak A., Snow T.P. (Eds.) 1987, in Physics of Be Stars, IAU Col. 92, Cambridge Univ. Press, Cambridge
Slipher V.M. 1903, Lowell Obs. Bull. 1, 4
Smith M.A. 1977, ApJ 215, 574
Smith M.A. 1978, ApJ 224, 927
Smith M.A. 1986, in Hydrodymanic and Magnetohydrodynamic Problems in the Sun and Stars, Ed. by Y. Osaki, Univ. of Tokyo, Tokyo, Japan, p. 145
Stebbins J. 1914, ApJ 39, 481
Vogt S.S., Penrod G.D. 1983, ApJ 275, 661
Walker G.A.H., Yang S., Fahlman G.G. 1979, ApJ 233, 199
Walker G.A.H., Yang S., Fahlman G.G. 1981, in Workshop On Pulsating B Stars, Ed. by G.E.V.O.N. & C. Sterken, Nice Obs. Publ., 261

This article was processed by the author using Springer-Verlag LaTeX A&A style file *L-AA* version 3.